Journal of Physical and Theoretical Chemistry
of Islamic Azad University of Iran, 14 (2) 111-126: Summer 2017
(J. Phys. Theor. Chem. IAU Iran)
ISSN 1735-2126

Quantum Chemical Modeling of 2-(Cyclohexylamino)-2-oxo-1-(quinolin-4-yl)ethyl 4-Chlorobenzoate: Molecular Structure, Spectroscopic (FT-IR, NMR, UV) Investigations, FMO, MEP and NBO Analysis Based on HF and DFT Calculations

Mehdi Nouri Angoran[1], Ali Ramazani[1,*] and Masoome Sheikhi[2]

[1] Department of Chemistry, Zanjan Branch, Islamic Azad University, Zanjan, Iran
[2] Young Researchers and Elite Club, Gorgan Branch, Islamic Azad University, Gorgan, Iran

Received August 2017; Accepted October 2017

ABSTRACT

In the present work, the quantum theoretical calculations of the molecular structure of the compound 2-(Cyclohexylamino)-2-oxo-1-(quinolin-4-yl)ethyl 4-Chlorobenzoate have been predicted using Density Functional Theory (DFT) in the gas phase. The geometry of the title structure was optimized by B3LYP/6-31+G* and HF/6-31+G* levels of theory. The theoretical ^{1}H and ^{13}C NMR chemical shift values of the title structure are calculated and compared with the experimental results. The calculated results are in good agreement with the experimental data. The theoretical vibrational frequencies values are obtained and compared with the experimental data. The electronic spectra of the title structure in the gas phase were carried out by TDB3LYP/6-31+G* and TDHF/6-31+G* levels of theory. Frontier molecular orbitals (FMOs), the molecular electrostatic potential (MEP), natural charges distribution (NBO charges), electronic properties such as ionization potential (I), electron affinity (A), global hardness (η), electronegativity (χ), electronic chemical potential (μ) and electrophilicity (ω), chemical softness ($S=1/\eta$), and NBO analysis were investigated and discussed by theoretical calculations.

Keywords: quinoline; DFT calculation; chemical shift; NBO analysis; electronic properties

INTRODUCTION

Quinoline is an organic compound including a double ring structure with one benzene ring and one pyridine ring that fused at two adjacent carbon atoms [1]. Quinoline derivatives have important applications such as in the field of inorganic chemistry as a ligand, electrochemical sensors, medicine, non-linear optics and optical switches [2-7]. Quinolines have been also used as inhibitor from corrosion of copper [8,9], steel [10,11], aluminum alloy [12] and magnesium [13]. Quinoline and its derivatives have biological activities such as antimalarial, anticancer, antibacterial, anticonvulsant, cardiotonic, antifungal, anthelmintic, anti-inflammatory and analgesic activity [14-18].

In recent years, computational chemistry has become an important tool for chemists and a well-accepted partner for experimental chemistry [19-21]. Density functional theory (DFT) method has become a major tool in the methodological arsenal of computational organic chemists. Dapeng and co-workers

[*]Corresponding author: aliramazani@gmail.com

[22] investigated effect two quinoline derivatives such as 8-aminoquinoline and 8-nitroquinoline on corrosion inhibition of aluminum alloy in based on DFT studies. The results confirmed that there is a strong hybridization between the sp-orbital of the Al atom in aluminum alloy and the p-orbital of reactive sites in the quinoline derivatives. Wazzan and co-workers reported DFT and TD-DFT studies of quinoline-3-carbonitrile dyes [23]. The results of their studies are shown charge transfer occur within the two compounds that are due to low HOMO-LUMO energy gaps and predicts that these compounds have bioactivity. The TD-DFT functional shows clearly the bathochromic shift that occurs between the absorption and emission spectra. Menon and co-workers [24] reported the synthesis and theoretical calculations of quinoline derivative by molecular dynamics simulations and DFT calculations. According to their studies, the calculated geometrical parameters are in agreement with the XRD data. We have previously been synthesized structure of 2-(Cyclohexylamino)-2-oxo-1-(quinolin-4-yl)ethyl 4-Chlorobenzoate [25]. In the current work, we modeled this compound by DFT and HF method and 6-31+G* basis set. The optimized geometry, spectroscopic (FT− IR, NMR, UV) investigations, frontier molecular orbitals, detail of quantum molecular descriptors, molecular electrostatic potential, natural charge and natural bond orbital analysis of the title compound were calculated.

COMPUTATIONAL METHODS

In this work, we have carried out quantum theoretical calculations and optimized structure of the compound 2-(Cyclohexylamino)-2-oxo-1-(quinolin-4-yl)ethyl 4-Chlorobenzoate using the DFT(B3LYP) [27] and HF method with 6-31+G* basis set by the Gaussian 09W program package [27] in the gas phase. The electronic properties such as E_{HOMO}, E_{LUMO}, HOMO-LUMO energy gap, dipole moment (μ_D), point group and natural charges were calculated [21]. The optimized structure, the shape of HOMO, and LUMO orbitals were obtained using GaussView 05 program [28]. We calculated NMR parameters such as ^{1}H and ^{13}C chemical shift (GIAO method) [29] and the theoretical IR spectra of the optimized structure using B3LYP/6-31+G* and HF/6-31+G* methods and were compared with experimental data. We were also used TD-DFT for computing the electronic transitions of the title structure. The theoretical absorption spectrum of the title compound in the gas phase was calculated using TDB3LYP/6-31+G* method. The electronic structure of the title compound was studied by using Natural Bond Orbital (NBO) analysis [19] using B3LYP/6-311+G* level of energy in order to understand hyperconjugation interactions and charge delocalization.

Optimized structure of the title compound

We have carried out quantum chemical calculations and have the optimized structure of the title compound using the DFT (B3LYP) and HF methods with 6-31+G* basis set by the Gaussian 09W program package (Fig. 1(b)). The title compound has C1 point group symmetry. The total energy of the title compound has been calculated by HF/6-31+G* and B3LYP/6-31+G* levels of energy, that are -1715.2991823 Hatree and-1723.8767398 Hatree, respectively.

The hydrogen bonds length values of experimental [25] and theoretical of the title compound summarized in Table 1. The first intramolecular hydrogen bonding of the title compound is C18-H38…O23. The experimental and theoretical values of bond length H38…O23 are 2.57Å and 2.59Å (HF and DFT) respectively, that

suggesting the existence of very strong intramolecular hydrogen bond. In another intramolecular hydrogen bonding is C3-[H31…O8], the experimental bond length H31…O8 is 2.58Å and calculated values are 3.92Å (HF) and 3.97Å (DFT).

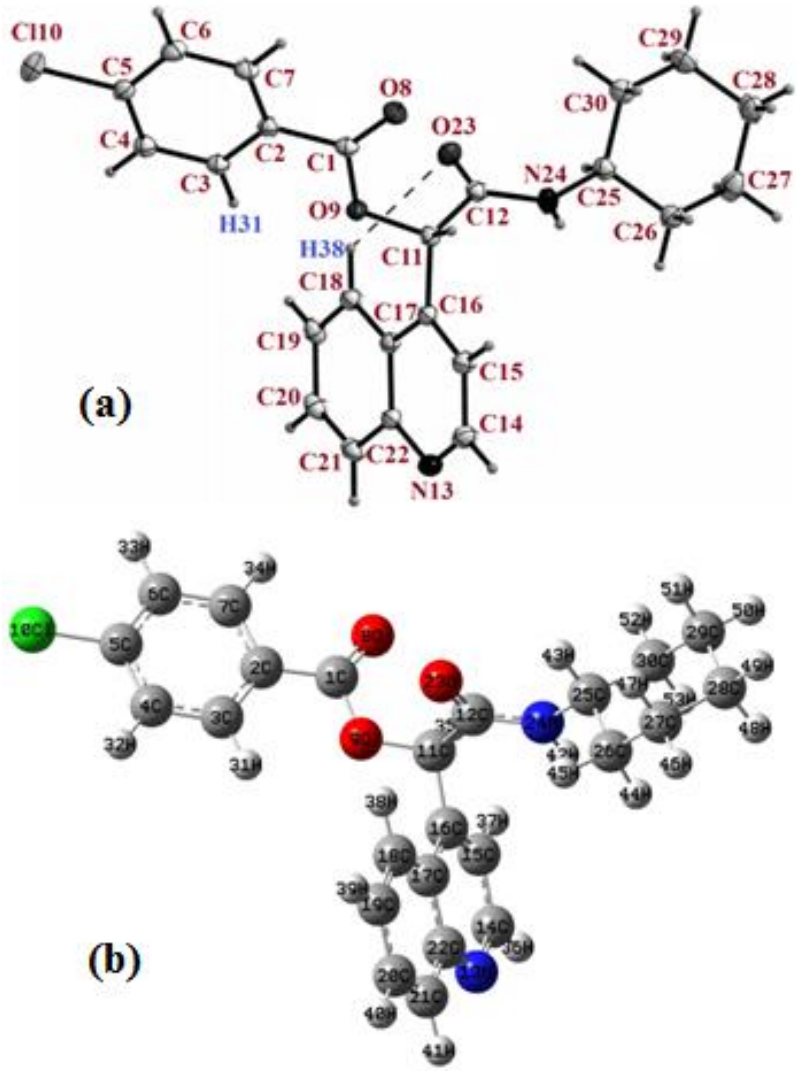

Fig. 1. (a) X-Ray crystal structure of the title compound (b) Optimized molecular structure of the title compound calculated by B3LYP/6-31+G* method.

Table 1. Hydrogen-Bond Geometry (Å) (Experimental and calculated by HF and B3LYP methods with 6-31+G* basis set) of the title compound

D-H…A	D-H (Å)			H…A(Å)			D…A(Å)		
	Exp.[a]	HF	B3LYP	Exp.[a]	HF	B3LYP	Exp.[a]	HF	B3LYP
C18-H38…O23	0.95	1.07	1.08	2.57	2.59	2.59	3.290(13)	3.461	3.477
C3-H31…O8	0.95	1.07	1.08	2.58	3.92	3.97	3.156(14)	3.614	3.65

[a] Taken from Ref. [25].

NMR chemical shift analysis

In the present study, the theoretical ^{1}H and ^{13}C NMR chemical shift values of the title compound were calculated by B3LYP/6-31+G* level of energy using the GIAO method. Then calculated ^{1}H and ^{13}C NMR chemical shifts were compared with the experimental values (Table 2). In the present study, the theoretical ^{1}H and ^{13}C NMR chemical shift values of the title compound were calculated by HF and B3LYP methods with 6-31+G* basis set using GIAO method. Then calculated ^{1}H and ^{13}C NMR chemical shifts compared with the experimental values (see Table 2). ^{1}H and ^{13}C NMR chemical shifts are reported in ppm relative to TMS. According to results, it can be seen a good agreement between experimental and calculated values. The difference between the theoretical and experimental values may be due to the fact that theoretical calculations of the title compound have been done in gas phase.

Table 2. The selected theoretical and experimental ^{1}H and ^{13}C chemical shifts of the title compound

Atoms	Theoretical		Experimental [a] ($CDCl_3$), Assignment
	HF/6-31+G*	B3LYP/6-31+G*	
^{1}HNMR			
H44-H53	0.5-1.44	0.2-1.62	1.13-1.69 (m, 5CH_2)
H43	3.35	4.00	3.81-3.90 (m, N-CH)
H42	3.11	3.76	6.11 (d, J = 8, NH)
H35	5.84	6.12	6.97 (s, CH-O)
H31	8.23	7.86	7.29-8.98 (m, 10 arom. H)
H32	7.31	6.96	
H33	7.47	7.15	
H34	8.69	8.11	
H36	9.02	8.83	
H37	7.27	6.81	
H38	8.70	8.54	
H39	7.72	7.44	
H40	7.92	7.71	
H41	8.49	8.14	
^{13}CNMR			
C26	28.87	29.50	24.66-32.84 (5 CH_2)
C27	20.88	20.04	
C28	21.23	20.04	
C29	21.64	19.99	
C30	27.96	29.49	
C25	40.38	41.97	48.75 (N-CH)
C11	66.45	68.71	72.94 (O-CH)
C2	123.74	114.66	126.10-148.43 (5 C)
C5	142.52	135.77	
C16	141.13	148.07	
C17	121.82	115.99	
C22	147.64	138.02	
C1	156.69	150.29	164.19 (ester C=O)
C12	161.57	150.8	165.94 (amid C=O)

[a] Taken from Ref. [25].

Electronic properties

Quantum chemical methods are important for obtaining information about molecular structure and electrochemical behavior of organic molecules. The frontier molecular orbitals (FMO) analysis plays an important role in the electronic properties and chemical reactions [31,32]. The HOMO and LUMO orbitals can act as the electron acceptor and electron donor. The FMO results of the title compound are summarized in Table 3. The graphical shapes of the HOMO and LUMO molecular orbitals of the title compound in the gas phase are shown in Fig. 2.

The HOMO-LUMO energy gap is an important parameter in determining molecular electrical transport properties and reactivity of the molecules. The increase of the HOMO-LUMO energy gap decreases the reactivity of the compound

Table 3. The calculated electronic properties of the title compound using the B3LYP/6-31+G* method

Property	**B3LYP**
E_{HOMO} (eV)	-6.74
E_{LUMO} (eV)	-2.1
Energy gap (eV)	4.64
Ionisation potential *I* (eV)	6.74
Electron affinity *A* (eV)	2.1
Electronegativity χ (eV)	4.42
Global hardness η (eV)	2.32
Chemical potential μ (eV)	-4.42
Global electrophilicity ω (eV)	4.21
Chemical softness *S* (eV^{-1})	0.43
Dipole moment (Debye)	3.3029

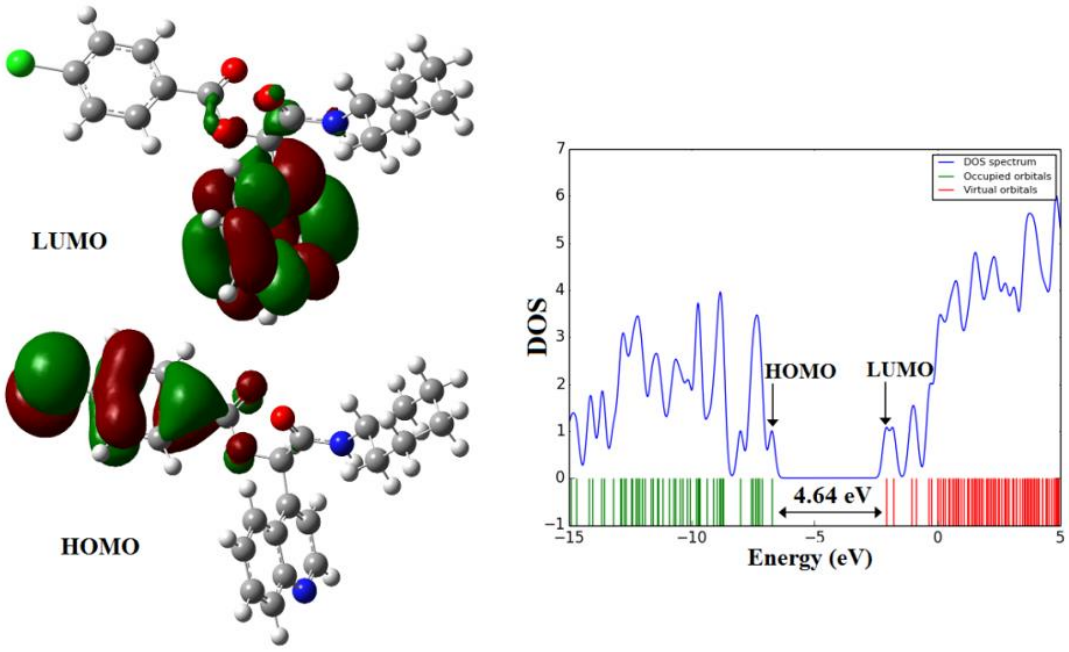

Fig. 2. Calculated Frontier molecular orbitals and DOS plot of the title compound by B3LYP/6-31+G* method.

that leads to increasing the stability of the compound [33]. Total electronic densities of states (DOSs) [31] of the compound was computed (Fig. 2). The DOS analysis indicates that the HOMO-LUMO energy gap of the title compound is about 4.64 eV at the B3LYP/6-31+G* level of energy.

The energy of HOMO (-6.74 eV) is directly related to the ionization potential ($I = -E_{HOMO}$), whereas the energy of LUMO (-2.1 eV) is related to the electron affinity ($A = -E_{LUMO}$). Also the global hardness ($\eta = I - A/2$), electronegativity ($\chi = I + A/2$), electronic chemical potential ($\mu = -(I+A)/2$) and electrophilicity ($\omega = \mu^2/2\eta$) [21], chemical softness ($S = 1/\eta$) [32] are calculated and is reported in Table 3 such as 2.32 eV, 4.42 eV, -4.42 eV, 4.21 eV and 0.43 eV^{-1}, respectively. The global hardness (η) corresponds to the HOMO-LUMO energy gap. A molecule with a small energy gap has high chemical reactivity, low kinetic stability and is a soft molecule, while a hard molecule has a large energy gap [19]. Electronegativity (χ) is a measure of the power of an atom or a group of atoms to attract electrons [34] and the chemical softness (S) describes the capacity of an atom or a group of atoms to receive electrons. Also, the dipole moment is a good measurement for the study of asymmetric nature of compounds. The value of dipole moment for the title compound is 3.3029 Debye (see Table 3). The magnitude of the dipole moment is related to the composition and dimensionality of the 3D compounds. The point group of the title compounds is C1, which refers to their high asymmetry.

Molecular electrostatic potential (MEP) of the title compound

Molecular electrostatic potential (MEP) maps show the electronic density and are useful in recognition of sites of negative and positive electrostatic potentials for electrophilic attack and nucleophilic reactions as well as hydrogen bonding interactions [35,36]. The difference of the electrostatic potential at the surface of the molecules is represented by different in color. The negative regions of MEP with the high electron density (red, orange and yellow color) were related to electrophilic reactivity, the positive regions (blue color) with the low electron density ones to nucleophilic reactivity and the green color is neutral regions. The MEP of the title compound were checked out by theoretical calculations using the B3LYP/6-31+G* level of energy (Fig. 3).

As shown in Fig. 3, the negative site (red color) of the title molecule is mainly focused on O8 and O23 atoms. Therefore, these positions are suitable for electrophilic attack. The areas of the title molecule with red or yellow colors such as phenyl and quinoline rings are sites with weak interaction. The H42 atom with blue color is the positive potential site, therefore, it is a suitable position for nucleophilic activity. Also, the regions with green color such as cyclohexane ring and chlorine atom show sites with zero potential.

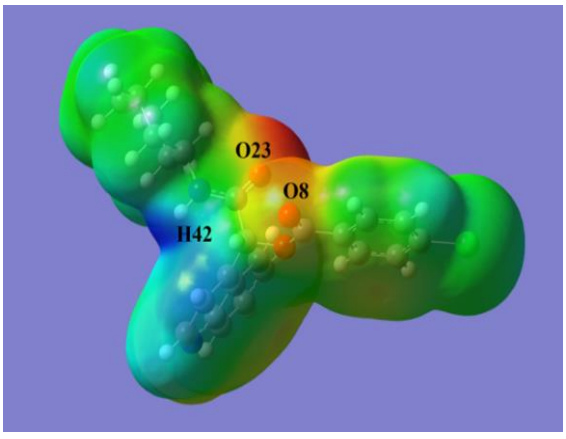

Fig. 3. Molecular electrostatic potential (MEP) map of the title compound calculated using the B3LYP/6-31+G* level of energy.

Natural charge analysis

The atomic charges have an important role in the electronic structure, molecular polarizability, dipole moment, and related properties of molecular systems. We calculated the natural charge distributions for the title molecule by the NBO analysis [21] using the B3LYP/6-31+G* and HF/6-31+G* levels of energy. The total charge of the investigated molecule is equal to zero. Fig. 4 shows results of natural charges (NBO) of the title compound in graphical form (Atoms numbering is according to Fig. 1(b)).

The results of the natural charge (NBO) analysis shows that carbon atoms have both positive and negative charges values. In fact, the carbons atoms attachment to the electron-withdrawing nitrogen and oxygen atoms (C1, C11, C12, C22) have the positive charges and the other carbon atoms have the negative charge. The C27 atom of the title compound has the highest negative charge rather than other carbon atoms. The highest positive charge in the title compound is observed for C1 atom (HF=0.996e and B3LYP=0.822e) due to attachment to the electron-withdrawing oxygen atoms (O8 and O23). The oxygen and nitrogen atoms of the title structure have a negative charge. According to Fig. 4, the highest negative charge in the compound is observed for N24 atom (HF=-0.741e and B3LYP=-0.654e). Natural charge's plot of the compound (Fig. 4) is shown all hydrogen atoms have the positive charge and H42 atom has the highest positive charge (HF=0.421e and B3LYP=0.424e) rather than other hydrogen atoms due to attachment to the electron-withdrawing N24, therefore it is acidic hydrogen.

NBO analysis

Natural bond orbital (NBO) analysis is an important method for studying intra- and inter-molecular bonding and interaction between bonds in molecular systems [37]. Electron donor orbitals, acceptor orbitals and the interacting stabilization energy ($E^{(2)}$) resulting from the second-order micro disturbance theory for the title compound are reported in Table 4.

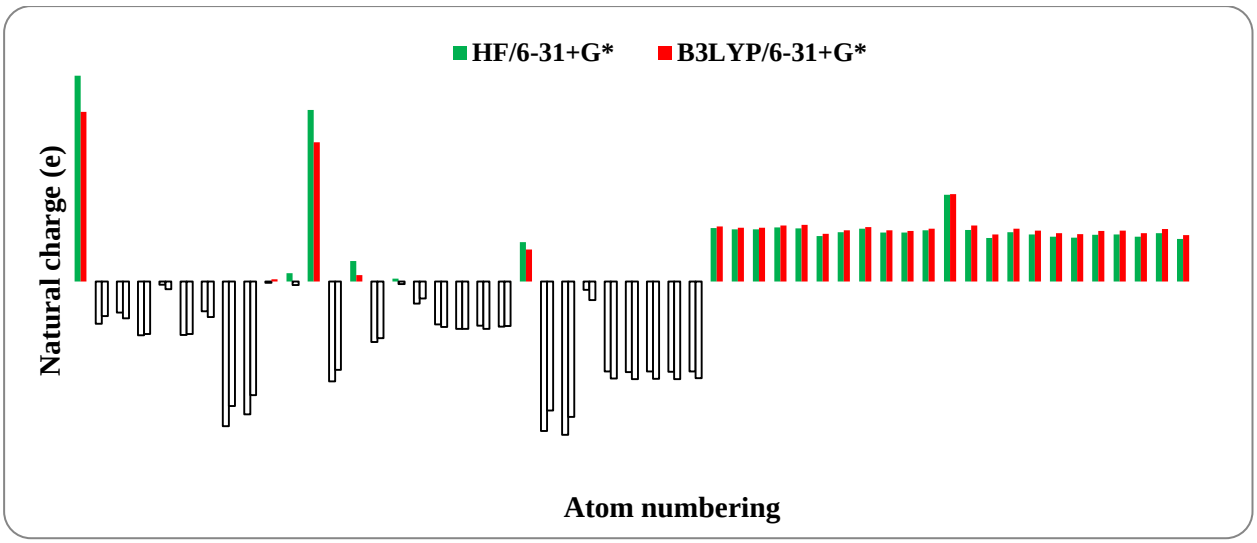

Fig. 4. Natural charges distribution of the title compound calculated by HF/6-31+G* and B3LYP/6-31+G* level of energy.

Table 4. Significant donor−acceptor interactions and second order perturbation energies of the title compound calculated using the B3LYP/6-31+G* level of energy

Donor (i)	Occupancy	Acceptor (j)	Occupancy	$E^{(2)a}$ kcal/mol	E(j)-E(i)[b] a.u.	F(i , j)[c] a.u.
π(C2-C3)	1.63303	π*(C1-O8)	0.25506	22.47	0.26	0.071
		π*(C4-C5)	0.38488	19.96	0.26	0.065
		π*(C6-C7)	0.29016	21.22	0.28	0.070
π(C4-C5)	1.66166	π*(C2-C3)	0.36920	20.39	0.30	0.070
		π*(C6-C7)	0.29016	16.95	0.30	0.064
π(C6-C7)	1.65435	π*(C2-C3)	0.36920	17.93	0.28	0.064
		π*(C4-C5)	0.38488	22.35	0.26	0.069
π(N13-C14)	1.78875	π*(C15-C16)	0.26202	11.39	0.33	0.055
π(C15-C16)	1.73016	π*(N13-C14)	0.28550	22.52	0.29	0.072
π(C18-C19)	1.72745	π*(C20-C21)	0.23830	17.05	0.29	0.064
π(C20-C21)	1.72505	π*(C18-C19)	0.24374	17.06	0.29	0.064
π*(C1-O8)	0.25506	π*(C2-C3)	0.36920	131.20	0.02	0.073
π*(C4-C5)	0.38488	π*(C2-C3)	0.36920	186.19	0.02	0.084
		π*(C6-C7)	0.29016	136.91	0.02	0.078
π*(N13-C14)	0.28550	π*(C15-C16)	0.26202	194.97	0.01	0.080
σ(C1-C2)	1.97370	σ*(O9-C11)	0.03901	3.35	0.94	0.050
σ(C3-C4)	1.97290	σ*(C4-C5)	0.02700	2.70	1.25	0.052
		σ*(C4-H32)	0.01213	1.16	1.16	0.033
		σ*(C5-Cl10)	0.02989	4.73	0.85	0.056
σ(C14-H36)	1.98245	σ*(N13-C22)	0.02120	5.01	1.03	0.064
		σ*(C15-C16)	0.01824	3.56	1.11	0.056
σ(C15-H37)	1.98029	σ*(C14-C15)	0.02818	0.58	1.07	0.022
		σ*(C15-C16)	0.01824	1.36	1.12	0.035
		σ*(C16-C17)	0.02988	4.85	1.07	0.065
σ(C17-C22)	1.97227	σ*(C11-C16)	0.02831	3.69	1.08	0.056
σ(C18-C19)	1.98097	σ*(C16-C17)	0.02988	3.52	1.24	0.059
σ(C18-H38)	1.97846	σ*(C17-C22)	0.04143	4.28	1.04	0.060
		σ*(C19-C20)	0.01655	4.13	1.06	0.059
σ(C19-H39)	1.98248	σ*(C17-C18)	0.02178	4.33	1.06	0.061
σ(N24-H42)	1.98247	σ*(C12-O23)	0.02055	5.63	1.25	0.075
		σ*(C25-H43)	0.02358	1.41	1.10	0.035
n1(O8)	1.97523	σ*(C1-C2)	0.06313	2.78	1.13	0.050
		σ*(C1-O9)	0.10513	1.50	1.05	0.036
n2(O8)	1.84306	σ*(C1-C2)	0.06313	18.22	0.70	0.103
		σ*(C1-O9)	0.10513	34.31	0.62	0.132
n1(O9)	1.95909	σ*(C1-O8)	0.01882	8.40	1.16	0.089
		σ*(C11-H35)	0.02508	2.79	0.99	0.047
n2(O9)	1.79926	π*(C1-O8)	0.25506	44.53	0.34	0.111
		σ*(C11-C12)	0.09704	7.26	0.66	0.063
n1(Cl10)	1.99229	σ*(C4-C5)	0.02700	1.58	1.47	0.043
		σ*(C5-C6)	0.02713	1.58	1.47	0.043
n2(Cl10)	1.97247	σ*(C4-C5)	0.02700	3.93	0.87	0.052
		σ*(C5-C6)	0.02713	3.93	0.86	0.052
n3(Cl10)	1.92393	π*(C4-C5)	0.38488	12.63	0.32	0.062
n1(N13)	1.91856	σ*(C14-C15)	0.02818	10.58	0.87	0.087
		σ*(C14-H36)	0.02128	2.95	0.79	0.044
		σ*(C17-C22)	0.04143	10.74	0.87	0.087
		σ*(C21-C22)	0.02299	1.57	0.88	0.034
n1(O23)	1.97542	σ*(C11-C12)	0.09704	1.92	1.01	0.040
		σ*(C12-N24)	0.06983	2.42	1.17	0.048
n2(O23)	1.85111	σ*(C11-C12)	0.09704	24.26	0.58	0.107
		σ*(C12-N24)	0.06983	23.76	0.73	0.120
		σ*(C25-H43)	0.02358	0.68	0.68	0.020
n1(N24)	1.69233	π*(C12-O23)	0.29756	66.10	0.28	0.122
		σ*(C25-C26)	0.02659	5.89	0.63	0.059

[a] E(2) Energy of hyperconjucative interactions,
[b] Energy difference between donor and acceptor i and j NBO orbitals,
[c] F(i, j) Is the Fock matrix element between i and j NBO orbitals.

The electron delocalization from filled NBOs (donors) to the empty NBOs (acceptors) describes a conjugative electron transfer process between them. For each donor (*i*) and acceptor (*j*), the stabilization energy $E^{(2)}$ associated with the delocalization $i \rightarrow j$ is estimated [38]:

$$E^{(2)} = \Delta E_{ij} = q_i \frac{F(i,j)^2}{\varepsilon_j - \varepsilon_i} \quad (1)$$

where q_i is the donor orbital occupancy, ε_j and ε_i are diagonal elements and F(i,j) is the off-diagonal NBO Fock matrix element. The resonance energy ($E^{(2)}$) detected the quantity of participation of electrons in the resonance between atoms. The larger $E^{(2)}$ value, the more intensive is the interaction between electron donors and acceptor, i.e. the more donation tendency from electron donors to electron acceptors and the greater the extent of conjugation of the whole system [37]. Delocalization of electron density between occupied Lewis-type (bond or lone pair) NBO orbitals and formally unoccupied (antibonding or Rydberg) non-Lewis NBO orbitals correspond to a stabilization donor–acceptor interaction. NBO analysis has been performed for the title compound at the B3LYP/6-31+G* level of energy in order to elucidate the intramolecular, rehybridization and delocalization of electron density within the title compound. The strong, moderate and weak intramolecular hyperconjugation interactions of the title compound such as π→π*, π*→π*, σ→σ*, n→σ* and n→π* transitions are presented in Table 4. According to NBO analysis, the σ(N24-H42)→σ*(C12-O23) transition has the highest resonance energy (5.63 kcal/mol) rather than other σ→σ* transitions of the title compound. The σ(C3-C4) orbital in phenyl ring participates as donor and the anti-bonding σ*(C4-C5), σ*(C4-H32) and σ*(C5-Cl10) orbitals act as acceptor with resonance energies ($E^{(2)}$) of is 2.70 kcal/mol, 1.16 kcal/mol, and 4.73 kcal/mol, respectively. These values indicate σ(C3-C4)→σ*(C5-Cl10) transition has the higher resonance energy (4.73 kcal/mol) rather than σ(C3-C4)→σ*(C4-C5) and σ(C3-C4)→σ*(C4-H32) transitions. The intramolecular hyperconjugation interactions of the π→π* transitions in phenyl ring that leads to a strong delocalization are such as C2-C3→C1-O8, C2-C3→C6-C7, C6-C7→C4-C5 and C15-C16→N13-C14 with resonance energies ($E^{(2)}$) 22.47 kcal/mol, 21.22 kcal/mol, 22.35 kcal/mol and 22.52 kcal/mol, respectively. The π*→π* transitions have the highest resonance energies compared with other interactions of the title compound such as C1-O8→C2-C3, C4-C5→C2-C3, C4-C5→C6-C7 and N13-C14→C15-C16 with resonance energies ($E^{(2)}$) 131.20 kcal/mol, 186.19 kcal/mol, 136.91 kcal/mol and 194.97 kcal/mol respectively, that lead to stability of the title compound. The strongest n→π* transitions are due to n2(O9)→π*(C1-O8) and n1(N24)→π*(C12-O23) interactions with stabilization energies of 44.53 kcal/mol and 66.10 kcal/mol respectively.

The results of NBO analysis such as the occupation numbers with their energies for the interacting NBOs [interaction between natural bond orbital A and natural bond orbital B (A-B)] and the polarization coefficient amounts of atoms in the title compound are presented using the B3LYP/6-31+G* method is summarized in Table 5 (Atoms labeling is according to Fig. 1(b)).

The size of polarization coefficients shows the importance of the two hybrids in the formation of the bond in a molecular system. The differences in electronegativity of the atoms involved in the bond formation are reflected in the larger differences in the polarization coefficients of the atoms. As can be seen

Table 5. Calculated natural bond orbitals (NBO) and the polarization coefficient for each hybrid in selected bonds of the title compound using the B3LYP/6-31+G* level of energy

Occupancy (a.u.)	Bond (A-B)[a]	Energy (a.u.)	ED_A (%)	ED_B (%)	NBO	S(%) (A)	S(%) (B)	P(%) (A)	P(%) (B)
1.99529	σ(C1-O8)	-1.09493	34.73	65.27	0.5893 ($sp^{1.93}$) + 0.8079 ($sp^{1.43}$)	34.06	40.90	65.84	58.68
1.98174	π(C1-O8)	-0.39125	29.63	70.37	0.5444 ($sp^{1.00}$) + 0.8389 ($sp^{1.00}$)	0.00	0.00	99.81	99.67
1.99018	σ(C1-O9)	-0.92080	30.74	69.26	0.5544 ($sp^{2.66}$) + 0.8322 ($sp^{2.15}$)	27.22	31.76	72.51	64.60
1.97588	σ(C2-C3)	-0.71487	51.29	48.71	0.7162 ($sp^{1.83}$) + 0.6979 ($sp^{1.92}$)	35.36	34.18	64.60	65.78
1.99021	σ(C5-Cl10)	-0.72487	45.73	54.27	0.6762 ($sp^{3.38}$) + 0.7367 ($sp^{4.75}$)	22.77	17.31	77.05	82.22
1.97295	σ(C6-C7)	-0.71687	50.36	49.64	0.7096 ($sp^{1.83}$) + 0.7046 ($sp^{1.84}$)	35.41	35.23	64.55	64.73
1.65435	π(C6-C7)	-0.26852	52.40	47.60	0.7239 ($sp^{1.00}$) + 0.6899 ($sp^{1.00}$)	0.00	0.00	99.96	99.95
1.99224	σ(C12-O23)	-1.05466	35.24	64.76	0.5937 ($sp^{2.07}$) + 0.8047 ($sp^{1.51}$)	32.57	39.65	67.34	59.96
1.98953	σ(C12-N24)	-0.84992	37.55	62.45	0.6128 ($sp^{2.00}$) + 0.7903 ($sp^{1.74}$)	33.28	36.42	66.59	63.55
1.98723	σ(N13-C14)	-0.85841	59.31	40.69	0.7701 ($sp^{1.69}$) + 0.6379 ($sp^{2.11}$)	37.04	32.11	62.75	67.82
1.78875	π(N13-C14)	-0.31766	57.98	42.02	0.7615 ($sp^{1.00}$) + 0.6482 ($sp^{1.00}$)	0.00	0.00	99.76	99.92
1.98248	σ(N13-C22)	-0.81043	58.02	41.98	0.7617 ($sp^{1.96}$) + 0.6479 ($sp^{2.33}$)	33.75	29.98	66.07	69.96
1.73016	π(C15-C16)	-0.28477	51.56	48.44	0.7180 ($sp^{1.00}$) + 0.6960 ($sp^{99.99}$)	0.00	0.02	99.95	99.93
1.97104	σ(C16-C17)	-0.70423	49.92	50.08	0.7066 ($sp^{1.97}$) + 0.7077 ($sp^{1.99}$)	33.64	33.44	66.32	66.53
1.97227	σ(C17-C22)	-0.69205	50.91	49.09	0.7135 ($sp^{2.13}$) + 0.7007 ($sp^{1.87}$)	31.89	34.86	68.06	65.09
1.98097	σ(C18-C19)	-0.71755	50.31	49.69	0.7093 ($sp^{1.78}$) + 0.7049 ($sp^{1.80}$)	35.99	35.69	63.97	64.27
1.98499	σ(N24-C25)	-0.74530	62.56	37.44	0.7909 ($sp^{1.85}$) + 0.6119 ($sp^{3.72}$)	35.04	21.15	64.94	78.71
1.97858	σ(C25-C26)	-0.59911	51.07	48.93	0.7146 ($sp^{2.63}$) + 0.6995 ($sp^{2.86}$)	24.51	25.90	72.45	72.55
1.97951	σ(C25-C30)	-0.60316	51.08	48.92	0.7147 ($sp^{2.65}$) + 0.6994 ($sp^{2.83}$)	27.41	26.07	72.55	73.88
1.98626	σ(C28-C29)	-0.59099	49.83	50.17	0.7059 ($sp^{2.75}$) + 0.7083 ($sp^{2.71}$)	26.64	26.93	73.31	73.03
1.98290	σ(C29-C30)	-0.59444	49.46	50.54	0.7033 ($sp^{2.78}$) + 0.7109 ($sp^{2.69}$)	26.46	27.09	73.49	72.87
1.96927	σ(C11-H35)	-0.54373	64.11	35.89	0.8007 ($sp^{2.81}$) + 0.5991 (s)	26.23	100	73.70	-
1.97847	σ(C3-H31)	-0.53825	63.42	36.58	0.7964 ($sp^{2.26}$) + 0.6048 (s)	30.61	100	69.34	-
1.97846	σ(C18-H38)	-0.53014	63.43	36.57	0.7964 ($sp^{2.23}$) + 0.6047 (s)	30.97	100	68.98	-
1.98247	σ(N24-H42)	-0.67696	71.76	28.24	0.8471 ($sp^{2.56}$) + 0.5314 (s)	28.06	100	71.89	-
1.97523	n1(O8)	-0.70820	-	-	$sp^{0.69}$	59.05	-	40.88	-
1.84306	n2(O8)	-0.27471	-	-	$sp^{1.00}$	0.01	-	99.72	-
1.95909	n1(O9)	-0.58329	-	-	$sp^{1.60}$	38.47	-	61.47	-
1.79926	n2(O9)	-0.33863	-	-	$sp^{99.99}$	0.09	-	99.82	-
1.99229	n1(Cl10)	-0.93625	-	-	$sp^{0.21}$	82.90	-	17.09	-
1.97247	n2(Cl10)	-0.33007	-	-	$sp^{1.00}$	0.00	-	99.98	-
1.92393	n3(Cl10)	-0.32879	-	-	$sp^{1.00}$	0.00	-	99.97	-
1.91856	n1(N13)	-0.35482	-	-	$sp^{2.42}$	29.15	-	70.69	-
1.97542	n1(O23)	-0.69461	-	-	$sp^{0.68}$	59.53	-	40.41	-
1.85111	n2(O23)	-0.25776	-	-	$sp^{99.99}$	0.03	-	99.73	-
1.69233	n1(N24)	-0.26637	-	-	$sp^{99.99}$	0.44	-	99.54	-

[a] A-B is a bond between atom A and atom B. (A: natural bond orbital and the polarization coefficient of atom; A-B: natural bond orbital and the polarization coefficient of atom B).

from Table 5, the calculated bonding orbital for the σ(C1-O8) bond is the $\sigma=0.5893(sp^{1.93})+0.8079(sp^{1.43})$ with high occupancy 1.99529a.u. and low energy -1.09493a.u. The polarization coefficients of C1=0.5893 and O8=0.8079 shows the importance of O8 in forming σ(C1-O8) bond compared with the C1 atom. The calculated bonding orbital for the σ(C12-N24) bond is

$\sigma=0.6128(sp^{2.00})+0.7903(sp^{1.74})$ is formed from $sp^{2.00}$ and $sp^{1.74}$ hybrids on C12 and N24 atoms which are the mixture of s(33.28%) p(66.59%) and s(36.42%) p(63.55%). Also in natural hybrid orbital π(C15-C16), the C15 and C16 atoms have p-character (99.95%) and (99.93%), respectively. From Table 5, it is found that the p-type orbital π(C15-C16) participates the electron donation to π*(N13-C14) in π(C15-C16)→π*(N13-C14) interaction with high resonance energies ($E^{(2)}$) 22.52 kcal/mol (see Table 4). According to NBO analysis, the natural hybrid orbital n2(O9) occupy a high energy orbital (-0.33863 a.u) with high occupation number (1.79926 a.u) and high p-character (99.82%). Therefore n2(O9) participates as electron donation to π*(C1-O8) in the n2(O9)→σ*(C1-O8) interaction with high resonance energies ($E^{(2)}$) 44.53 kcal/mol in the title compound (see Table 4). The natural hybrid orbital n1(N24) with occupancy 1.69233 a.u. and high energy -0.26637 a.u. has *p*-character (99.54%). Therefore pure p-type lone pair orbital n1(N24) participates as electron donation to π*(C12-O23) in the n1(N24)→π*(C12-O23) interaction with high resonance energy ($E^{(2)}$) 66.10 kcal/mol (see Table 4).

Vibrational frequencies

Harmonic vibrational frequencies of the optimized compound were calculated using the B3LYP/6-31+G* and HF/6-31+G* levels of energy. The vibrational frequencies assignments were predicted using the GaussView05 program. The theoretical frequencies calculated by DFT and HF methods are usually higher than the corresponding experimental data due to the approximate treatment of the electron correlation, anharmonicity effects and basis set deficiencies [39]. The important calculated and experimental vibrational frequencies of the title compound are summarized in Table 6. The C=C aromatic ring stretching vibrations are expected in the range 1650-1200 cm^{-1} [40]. As can be seen from Table 6, the C=C stretching vibrations of the title compound was assigned in the region 1569 cm^{-1} and the corresponding theoretical vibrations with HF and DFT methods is predicted in the region 1786 cm^{-1} and 1615 cm^{-1}. The C-H aromatic bending vibrations out of the plane are appeared in the region 1000-700 cm^{-1} [38]. The symmetric C–H stretching vibrations of the aromatic ring are assigned at of 3271 cm^{-1} and corresponding theoretical value appears at 3398 cm^{-1} (HF) and 3237 cm^{-1} (DFT). The theoretical IR spectra of the title compound for C-H aromatic stretching vibrations out of plane show a band at 1105 cm^{-1}, 990 cm^{-1}, 864 cm^{-1}, 856 cm^{-1} with HF method and 1009 cm^{-1}, 984 cm^{-1}, 862 cm^{-1}, 788 cm^{-1} with DFT method. The aryl-chloride (aryl C-Cl) stretching vibrations are expected in the ranges 1100-1035 cm^{-1}. The calculated C-Cl stretching vibration of the title compound with HF and DFT methods is observed at 1196 cm^{-1} and 1104 cm^{-1} respectively. The C-O stretching mods are expected in the range 1260-1000 cm^{-1}. The IR spectrum of the compound for the C-O stretching vibration show a band at 1095 cm^{-1} and the corresponding theoretical values are 1263 (HF) cm^{-1} and 1128 cm^{-1} (DFT). The C=O stretching vibrations in esters are expected in the region 1750-1735 cm^{-1}. According to experimental results, the C=O vibration of is observed in the region 1734 cm^{-1}. This stretching is assigned at 1972 and 1780 cm^{-1} by HF and B3LYP methods.

According to results, the calculated frequencies by B3LYP/31+G* method are closer to the experimental frequencies rather than HF/6-31+G* level of theory.

Electronic Structure and the Excited States of the title compound

We used the Time-dependent density

functional theory (TD-DFT) for predicting the absorption spectra of the title compound. The theoretical absorption spectrum of the optimized compound was calculated in the gas phase using the TDB3LYP/6-31+G* level of theory. We considered 20 excited states and the accurate value of absorption wavelength is obtained using the TD-DFT method (see Table 7).

According to theoretical calculations, the strong peak at λ_{max} = 249 nm and the oscillator strength f = 0.15 in electronic absorption spectrum of the title compound is due to Charge-Transfer of one electron into the excited singlet state $S_0 \rightarrow S_{11}$, which it describes by a wave function including five configurations [(H-5→L+1), (H-4→L+1), (H-3→L+1), (H-2→L+1), (H-1→L+1)] (Fig. 5). The transition from HOMO-2 to LUMO+1 (H-2→L+1) is main responsible for formation maximum wavelength at 249 nm (see Table 7). According to Fig. 5, the electron density of HOMO-1 is mainly focused on chlorine atom and the electron density of LUMO is mainly focused on double bonds (-C=C-) of the phenyl ring and (C=O) carbonyl group. Therefore the electronic transition from the HOMO-1 to LUMO+1 is due to the contribution of lone pair and pi (π) bonds (n→π*). The electron density of HOMO-2, HOMO-3, HOMO-4 is mainly focused on double bonds (-C=C-) of quinoline ring and (C=O) carbonyl group and the electron density of HOMO-5 is mainly focused on double bonds (-C=C-) of quinoline ring. Therefore the electronic transition from the HOMO-2, HOMO-3, HOMO-4, HOMO-5 to LUMO+1 is due to the contribution of pi (π) bonds (π→π*). The other important excited state is $S_0 \rightarrow S_{20}$ at 221 nm (f = 0.32) with five configurations for electronic excitations [(H-4→L+2), (H-3→L+1), (H-3→L+2), (H-2→L+2), (H→L+2)]. The other excited states of the title compound have very small intensity (f ≈ 0) that is nearly forbidden by orbital symmetry considerations (Table 7). The calculated UV−Vis spectrum of the title compound in the gas phase is observed in Fig. 6.

Table 6. Experimental and calculated vibrational frequencies of the title compound by HF/6-31+G* and B3LYP/6-31+G* level

$\nu_{exp.}$ (cm^{-1}) [a]	HF		B3LYP		Vibrational assignment
	$\nu_{cal.}$ (cm^{-1})	IR intensity	$\nu_{cal.}$ (cm^{-1})	IR intensity	
3445	3856	22.71	3581	12.44	ν(N-H)
3271	3398	12.82	3237	1.00	ν_{sym} (C-H)aromatic
2932	3186	55.12	3011	21.25	ν_{sym}(C-H)aliphatic
2851	3178	21.40	3002	16.75	ν_{sym}(C-H)aliphatic
1734	1972	360.01	1780	208.98	ν(C=O)
1700	1931	362.61	1760	316.75	ν(C=O)
1569	1786	35.26	1615	18.62	ν(C=C, C=N)aromatic
-	1760	8.90	1618	5.52	ν(C=C)aromatic
-	1679	28.74	1638	30.31	ν(C=C, C=N)aromatic
1253	1314	1.58	1303	5.79	β(C-H)aromatic
1095	1263	257.03	1128	367.30	ν(C-O)
-	1196	43.59	1104	80.18	ν(C-Cl)
-	1105	0.23	1009	0.66	ω (C-H)aromatic
-	990	1.32	984	0.94	ω (C-H) aromatic
-	864	38.07	862	21.53	ω (C-H) aromatic
-	856	64.53	788	66.79	ω (C-H) aromatic

Abbreviations: ν, stretching; β, in-plane bending; ω, out of plane bending; asym, asymmetric deformation.
[a] Taken from Ref. [25].

Table 7. The electronic absorption spectrum of the title compound calculated by TDB3LYP/6-31+G*

Excited State	Wavelength (nm)	Excitation Energy (eV)	Configurations Composition (corresponding transition orbitals)	Oscillator Strength (f)
S_1	299	4.14	0.11(H-5→L) + 0.10(H-4→L) + 0.10(H-3→L+2) + 0.66(H→L)	0.08
S_2	296	4.17	0.42(H-5→L) + 0.44(H-4→L) + 0.17(H-3→L) + 0.16(H-2→L) + 0.14(H-51L) - 0.16(H→L)	0.00
S_3	281	4.40	0.45(H-3→L) - 0.34 (H-2→L) - 0.40(H→L+2)	0.01
S_4	278	4.44	0.70(H→L+1)	0.00
S_5	274	4.51	- 0.18(H-5→L) - 0.19(H-4→L) + 0.29(H-3→L) + 0.51(H-2→L) + 0.25(H-1→L)	0.00
S_6	268	4.61	- 0.25(H-5→L) + 0.19(H-4→L) - 0.24(H-2→L) + 0.56(H-1→L)	0.01
S_7	262	4.73	- 0.42(H-5→L) + 0.43(H-4→L) + 0.11(H-3→L) - 0.30(H-1→L)	0.01
S_8	258	4.80	- 0.36(H-7→L+1) - 0.14(H-5→L+1) + 0.20(H-4→L+1) + 0.12(H-3→L+1) + 0.40(H-2→L+1) + 0.31(H-1→L+1)	0.05
S_9	253	4.88	- 0.11(H-7→L+1) - 0.19(H-6→L) + 0.52(H-6→L+1) - 0.36(H-1→L+3)	0.00
S_{10}	251	4.93	- 0.14(H-7→L) + 0.50(H-7→L+1) + 0.15(H-3→L+1) + 0.32(H-2→L+1) + 0.22(H-1→L+1)	0.03
S_{11}	249	4.97	0.14(H-5→L+1) - 0.29(H-4→L+1) - 0.11(H-3→L+1) + 0.44(H-2→L+1) - 0.38(H-1→L+1)	0.15
S_{12}	245	5.06	- 0.18(H-6→L) + 0.59(H-3→L+1) - 0.27(H-1→L+1)	0.08
S_{13}	244	5.07	0.57(H-6→L) + 0.12(H-6→L+1) + 0.10(H-5→L+1) - 0.22(H-4→L+1) + 0.24(H-3→L+1)	0.00
S_{14}	243	5.09	- 0.25(H-7→L) + 0.46(H-7→L+1) + 0.21(H-6→L) + 0.17(H-6→L+1) - 0.12(H-5→L+1) + 0.50(H-4→L+1) - 0.26(H-3→L+1) + 0.22(H-2→L+1) - 0.13(H-1→L+1)	0.10
S_{15}	239	5.18	0.44(H-5→L+2) + 0.46(H-4→L+2) + 0.17(H-3→L+2) + 0.16(H-2→L+2) + 0.14(H-1→L+2)	0.00
S_{16}	235	5.26	0.61(H-5→L+1) + 0.31(H-4→L+1)	0.00
S_{17}	231	5.34	0.65(H-7→L) - 0.19(H-7→L+1)	0.02
S_{18}	229	5.41	0.70(H→L+3)	0.00
S_{19}	225	5.50	0.28(H-5→L+2) + 0.13(H-4→L+4) - 0.14(H-3→L+4) - 0.12(H-8→L) - 0.12(H-4→L+2) - 0.22(H-1→L+2) - 0.21(H-1→L+2) - 0.19(H-1→L+2) - 0.21(H→L+4)	0.05
S_{20}	221	5.58	- 0.24(H-4→L+2) - 0.16(H-3→L) + 0.11(H-3→L+2) + 0.53(H-2→L+2) - 0.25(H→L+2)	0.12

*H-HOMO, L-LUMO

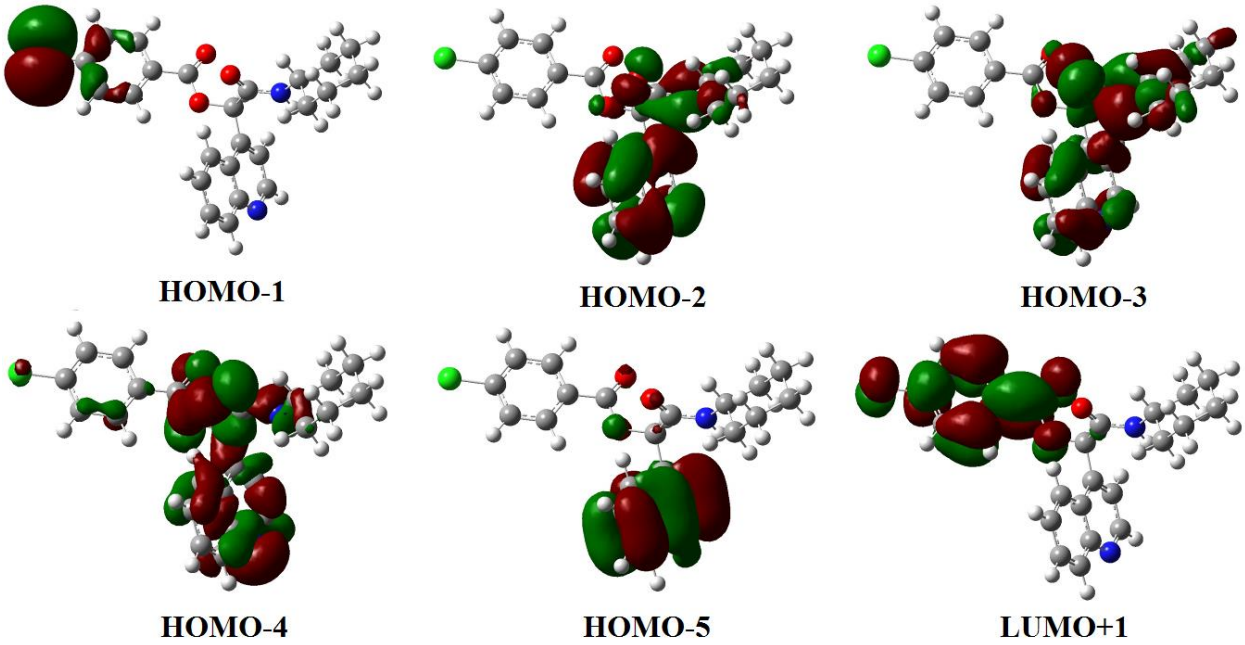

Fig. 5. The form of the MO involved in the formation of the absorption spectrum of the title compound at λ_{max} = 249 nm calculated by B3LYP/6-31+G* method.

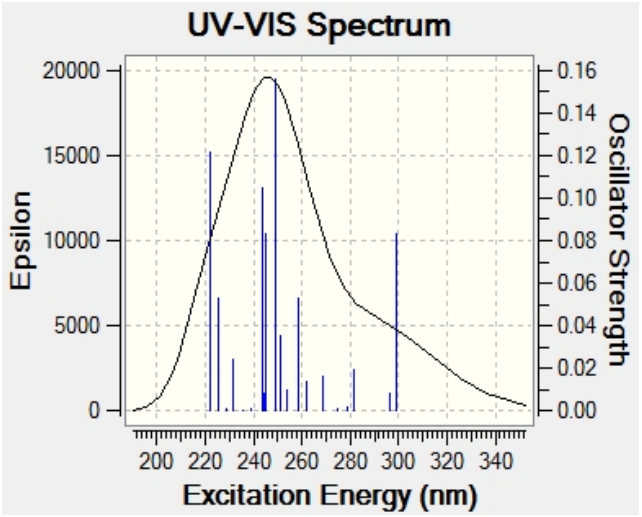

Fig. 6. UV-Vis spectrum of the title compound in gas phase calculated by B3LYP/6-31+G* method

CONCLUSION

In the present work, the electronic structure of the compound 2-(Cyclohexylamino)-2-oxo-1-(quinolin-4-yl)ethyl 4-Chlorobenzoate was optimized using the DFT and HF methods. According to results of ^{1}H and ^{13}C NMR chemical shift, the experimental values are in good agreement with the calculated values. From FMO analysis was found charge transfer is taking place within the structure. MEP map was shown the negative potential site of the title structure is oxygen atoms of the carbonyl groups (O8 and O23) and the positive potential site is the

H42. According to NBO analysis of the title compound, the highest resonance energy was observed for π*(N13-C14)→π*(C15-C16) transition and the strongest n→π* interaction is due to n1(N24)→π*(C12-O23) transition. The calculated frequencies by B3LYP/31+G* method are closer to the experimental frequencies rather than HF/6-31+G* level of theory. Investigation calculated electronic spectra of the title compound was shown compound has the highest λ_{max} in 249 nm due to Charge-Transfer of one electron into the excited singlet state $S_0 \rightarrow S_{11}$.

REFERENCES

[1] A. Marella, O. P. Tanwar, R. Saha, M. R. Ali, S. Srivastava, M. Akhter, M. Shaquiquzzaman and M.M. Alam, Saudi Pharm. J. 21 (2013) 1.

[2] S. A. Khan, A. M. Asiri, S. H. Al-Thaqafy, H. M. Faidallah and S.A. El-Daly, Spectrochim. Acta A 133 (2014) 141.

[3] P. Zhang, E. Terefenko, J. Kern, A. Fensome, E. Trybulski, R. Unwalla, J. Wrobel, S.Lockhead, Y. Zhu, J. Cohen, M. LaCava, R.C. Winneker and Z. Zhang, Bioorg. Med. Chem. 15 (2007) 6556.

[4] C. B. Sangani, J. A. Makawana, X. Zhang, S. B. Teraiya, L. Lin and H. L. Zhu, Eur. J. Med. Chem. 76 (2014) 549.

[5] M. Ghashang, S. S. Mansoor and K. Aswin, J. Adv. Res. 5 (2014) 209.

[6] W. Hamaguchi, N. Masuda, S. Miyamoto, Y. Shiina, S. Kikuchi, T. Mihara, H. Moriguchi, H. Fushiki, Y. Murakami, Y. Amano, K. Honbou and K. Hattori, Bioorg. Med. Chem. 23 (2015) 297.

[7] J. Taltavull, J. Serrat, J. Gràcia, A. Gavaldà, M. Córdoba, E. Calama, J. L. Montero, M. Andrés, M. Miralpeix, D. Vilella, B. Hernández, J. Beleta, H. Ryder and L. Pagès, Eur. J. Med. Chem. 46 (2011) 4946.

[8] M. Cubillos, M. Sancy, J. Pavez, E. Vargas and R. Urzua, Electrochim. Acta 55 (2010) 2782.

[9] G.P. Cicileo, B.M. Rosales, F.E. Varela and J.R. Vilche, Corros. Sci. 40 (1998)1915.

[10] G. Achary, H. P. Sachin, Y. A. Naik and T. V. Venkatesha, Mater. Chem. Phys. 107 (2008) 44.

[11] L. Tang, X. Li, Y. Si, G. Mu and G. Liu, Mater. Chem. Phys. 95 (2006) 29.

[12] S. V. Lamaka, M. L. Zheludkevich, K. A. Yasakau, M. F. Montemor and M. G. S. Ferreira, Electrochim. Acta 52 (2007) 7231.

[13] H. Gao, Q. Li, Y. Dai, F. Luo and H. X. Zhang, Corros. Sci. 52 (2010) 1603.

[14] B. N. Acharya, D. Thavaselvam and M. B. Kaushik, Med. Chem. Res. 17 (2008) 487.

[15] H. Assefa, S. Kamath and J. K. Buolamwini, J. Comput. Aided Mol. Des. 17 (2003) 475.

[16] A. Baba, N. Kawamura, H. Makino, Y. Ohta, S. Taketomi and T. Sohda, J. Med. Chem. 39 (1996) 5176.

[17] M. I. F. Bachiller, C. Perez, G. C. G. Munoz, S. Conde, M. G. Lopez, M. Villarroya, A. G. Garcia and M.I.R. Franco, J. Med. Chem. 53 (2010) 4927.

[18] M. Bingul, O. Tan, C. R. Gardner, S. K. Sutton, G. M. Arndt, G. M. Marshall, B. B. Cheung, N. Kumar and D. C. Black, Molecules 21 (2016) 916.

[19] S. Shahab, M. Sheikhi, L. Filippovich, E. Dikusar Anatol'evich and H. Yahyaei, J. Mol. Struct. 1137 (2017) 335.

[20] a) S. M. Shoaei, A.R. Kazemizadeh and A. Ramazani, Chin. J. Struct. Chem. 30 (2011) 568. b) A. Ramazani, A. Rouhani, E. Mirhadi, M. Sheikhi,

K. Ślepokura and T. Lis, Nano. Chem. Res. 1 (2016) 87.
[21] M. Sheikhi, D. Sheikh and A. Ramazani, S. Afr. J. Chem. 67 (2014) 151.
[22] D. Wang, D. Yang, D. Zhang, K. Li, L. Gao and T. Lin, App. Surf. Sci. 357 (2015) 2176.
[23] N. A.Wazzan, O. S. Al-Qurashi and H. M. Faidallah, J. Mol. Liq. 223 (2016) 29.
[24] V. V. Menon, E. Fazal, Y. S. Mary, C. Y. Panicker, S. Armakovic, S. J. Armakovic , S. Nagarajan and C. V. Alsenoy , J. Mol. Struct. 1127 (2017) 124.
[25] J. Tarana, A. Ramazani, S. W. Joo, K. Slepokurac and T. Lis, Helvetica Chimica. Acta 97 (2014) 1088.
[26] A. D. Becke, Density-functional thermochemistry. III. The role of exact exchange, J. Chem. Phys. 98 (1993) 5648.
[27] M. J. Frisch, G. W. Trucks, H. B. Schlegel, G. E. Scuseria, M. A. Robb, J. R. Cheeseman, G. Scalmani, V. Barone, B. Mennucci, G. A. Petersson, H. Nakatsuji, M. Caricato, X. Li, H. P. Hratchian, A. F. Izmaylov, J. Bloino, G. Zheng, J. L. Sonnenberg, M. Hada, M. Ehara, K. Toyota, R. Fukuda, J. Hasegawa, M. Ishida, T. Nakajima, Y. Honda, O. Kitao, H. Nakai, T. Vreven, J. A. Montgomery, Jr., J. E. Peralta, F. Ogliaro, M. Bearpark, J. J. Heyd, E. Brothers, K. N. Kudin, V. N. Staroverov, R. Kobayashi, J. Normand, K. Raghavachari, A. Rendell, J. C. Burant, S. S. Iyengar, J. Tomasi, M. Cossi, N. Rega, J. M. Millam, M. Klene, J. E. Knox, J. B. Cross, V. Bakken, C. Adamo, J. Jaramillo, R. Gomperts, R. E. Stratmann, O. Yazyev, A. J. Austin, R. Cammi, C. Pomelli, J. W. Ochterski, R. L. Martin, K. Morokuma, V. G. Zakrzewski, G. A. Voth, P. Salvador, J. J. Dannenberg, S. Dapprich, A. D. Daniels, Ö. Farkas, J. B. Foresman, J. V. Ortiz, J. Cioslowski and D. J. Fox, Gaussian, Inc., Wallingford CT, 2009.
[28] A. Frisch, A. B. Nielson and A. J. Holder, GAUSSVIEW User Manual, Gaussian Inc., Pittsburgh, PA, 2000.
[29] M. Sheikhi, E. Balali and H.Lari, J. Phys. Theor. Chem. 13 (2016) 155.
[30] B. D. Joshi, P. Tandon and S. Jain, The Himalayan Physics. 3 (2012) 44.
[31] M. Sheikhi and D. Sheikh, Rev. Roum. Chim. 59 (2014) 761.
[32] M. Sheikhi and S. Shahab, J. Phys. Theor. Chem. 13 (2016) 277.
[33] M. Khaleghian, F. Azarakhshi and M. Sheikhi, J. Phys. Theor. Chem. 13 (2016) 147-153.
[34] R. G. Parr and W. Yang, J. Am. Chem. Soc. 106 (1984) 4049.
[35] M. Sheikhi, V. Ranjbar and A. Ramazani, J. Phys. Theor. Chem. 13 (2017) 387.
[36] L. Shiri, D. Sheikh and M. Sheikhi, Rev. Roum. Chim. 59 (2014) 825.
[37] M. Monajjemi and M. Sheikhi, J. Phys. Theor. Chem. 8 (2017) 119.
[38] F. Weinhold and C. R. Landis, Natural Bond Orbitals and Extensions of Localized, 2001.
[39] H. Tanak, J. Phys. Chem. A. 115 (2011) 5133.
[40] L. J. Bellamy, The Infrared Spectra of Complex Molecules, 3rd ed., Wiley, New York, 1975.